Research Article | Vol. 28, No. 10 / 11 May 2020 / Optics Express 15294

Optics EXPRESS

Passive polymer-dispersed liquid crystal enabled multi-focal plane displays

ZIQIAN HE, KUN YIN, AND SHIN-TSON WU*

College of Optics and Photonics, University of Central Florida, Orlando, FL 32816, USA
**swu@creol.ucf.edu*

Abstract: A multi-focal plane see-through near-eye display using a transparent projection display is demonstrated. The key component of the transparent projection display is a passive polymer-dispersed liquid crystal (PDLC), which is highly transparent for a large range of incident angles in air but strongly scattering at large oblique angles in high refractive index medium (e.g. glass). The use of a passive device can avoid temporal multiplexing. Such a display is highly transparent in air and can easily deliver full-color images. The proposed method is an important step toward transparent display-enabled multi-focal plane displays.

1. Introduction

Thanks to the flourish of optics and electronics over the past decades, virtual reality (VR) and augmented reality (AR) displays have recently ushered in a renaissance. Although VR/AR has been heavily developed for years, it is still quite challenging to provide immersive, realistic and comfortable user experience [1,2]. One of the major challenges is the vergence-accommodation conflict (VAC) [3,4]. For most existing head-mounted displays (HMDs), the depth perception is generated by binocular disparity, where two different images are delivered to the observer's left and right eyes. While the vergence distance is varying according to different image contents, the accommodation distance is fixed at the display screen. This mismatch can result in visual discomfort and fatigue [5,6].

To overcome the VAC issue, several methods have been proposed, such as multi-focal plane (MFP) displays [7–12], vari-focal plane displays [13–15], integral imaging-based displays [16,17], and holographic displays [18,19]. The MFP displays can render correct or nearly correct focus cues with acceptable computation load, and thus have been investigated extensively. Transparent display stack, proposed by Rolland et al, is an interesting way to achieve MFP [20]. However, there will be a tradeoff between transparency and display brightness, and the use of multiple transparent screens can hardly deliver good image quality. Instead, Lee et al. demonstrated a projection-type transparent display stack using diffuser holographic optical elements (DHOEs) with very high average transmittance (~90%) [21]. However, the DHOE is restricted by Bragg diffraction condition and thus strongly dependent on wavelength. The working band can be multiplexed, but at the cost of diffraction efficiency. On the other hand, transparent projection display (TPD) stacks based on switchable scattering shutters using space-time multiplexing have been proposed [22,23]. Good image quality and decent scattering efficiency can be achieved, but the burden on frame rate will be heavy when increasing the stack numbers.

In this paper, we demonstrate an MFP display with passive polymer-dispersed liquid crystal (PDLC) films. As the key component, the passive PDLC is highly transparent for a large range of incident angles in air, but strongly scattering at large angles in high refractive index medium (e.g. glass). To prove concept, a birdbath architecture is applied to demonstrate a dual-plane (one TPD and one liquid crystal display (LCD)) see-through near-to-eye display. The large angle scattering of the passive PDLC is not restricted by Bragg condition and thus is intrinsically broadband. Meanwhile, the introduction of passive devices can effectively avoid temporal multiplexing.

#392489 https://doi.org/10.1364/OE.392489
Journal © 2020 Received 11 Mar 2020; revised 20 Apr 2020; accepted 24 Apr 2020; published 5 May 2020

Optics EXPRESS

2. System design

Figure 1(a) illustrates our proof-of-principle system, where a birdbath architecture is utilized. Two displays, one non-projection display (denoted as display panel 1 in Fig. 1(a)) and one PDLC-based TPD, are employed to generate two planes. The projected image on PDLC is coupled through a dove prism. The visual effect of the passive PDLC is shown in Fig. 1(b) and 1(c). The PDLC is highly transparent at the normal view (Fig. 1(b)), while it is scattering when looking through the sloped surface of the prism (Fig. 1(c)). This special angular selective scattering property ensures that displays behind the PDLC are clear and, in the meantime, the projector can form an image on the PDLC. Here, only two planes are illustrated. However, in principle, more planes can be created by stacking more PDLC TPDs. By doing so, the thickness of the TPD will be important for mapping the depth accurately. Here the thickness is primarily determined by the prism. To construct more planes, a thin lightguide can be used to allow multiple total internal reflections before forming the image on the PDLC.

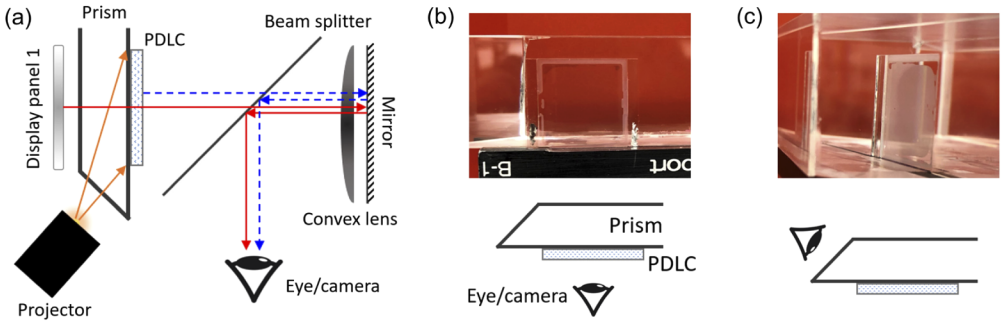

Fig. 1. (a) Schematic illustration of the dual-plane display using a birdbath architecture. The key component here is the angle-selective scattering passive PDLC. The PDLC is (b) highly transparent at the normal angle but (b) scattering at large oblique angles.

3. Passive PDLC with angle-selective scattering

3.1. Mechanism

Traditionally, PDLCs are applied as scattering-type optical shutters, either in normal mode (switching from scattering state to transparent state) or reverse mode (switching from transparent state to scattering state). In a normal-mode PDLC, the LC directors are arranged as micron-sized droplets dispersed in the polymer matrix by phase separation [24]. Within each droplet, the LCs are aligned in a certain direction to minimize the free energy. However, at the voltage-off state, the LC alignment direction varies from droplet to droplet, causing light scattering macroscopically. In the presence of a sufficiently high voltage, all the droplets are aligned along the vertical direction, and the PDLC is switched to a transparent state [25,26]. Selective scattering will be observed in such a state, where the normal incidence shows high transmittance and the scattering becomes stronger as the incident angle increases [27,28]. This selective-scattering property is leveraged in our case. The difference is that the transparent state needs to be maintained without voltage applied. The aligned PDLC can be obtained by adding reactive mesogen into PDLC precursors and curing the precursors in a thin vertical alignment (VA) cell with voltage applied [29,30].

The birefringent nature of LCs renders the PDLC both angle and polarization dependency. As shown in Fig. 2(a), ideally the *s*-polarized light will always see the ordinary refractive index of LCs (n_o) and the refractive index of the polymer (n_p). Since in this case they are nearly matched ($n_o \approx n_p$), the *s*-polarized light will not be scattered. In contrast, the *p*-polarized light (Fig. 2(b))

Optics EXPRESS

sees the effective refractive index of the LC (n_{eff}) and the n_p of the polymer, where n_{eff} can be calculated using n_o, n_e (the extraordinary refractive index of the LC), and incident angle (α) as:

$$n_{eff} = \frac{n_o n_e}{\sqrt{n_e^2 \cos^2\alpha + n_o^2 \sin^2\alpha}}. \quad (1)$$

At the normal incidence ($\alpha = 0$), the p-polarized light sees n_o ($n_{eff} = n_o$) of LC and n_p of the polymer, and thus will not be scattered. At larger oblique angles, the mismatch between n_{eff} and n_p becomes more significant, causing stronger light scattering.

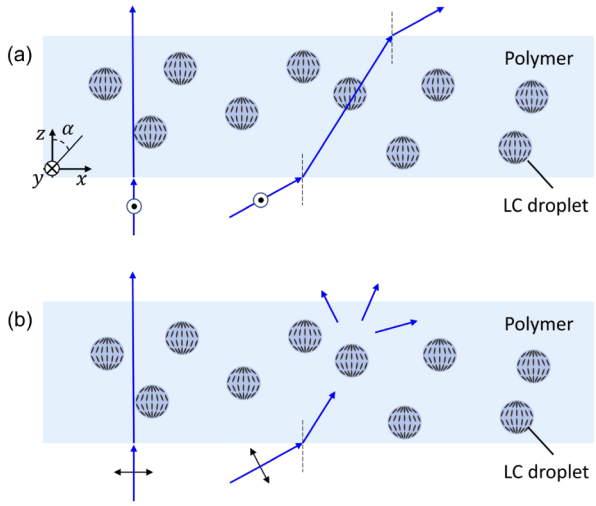

Fig. 2. Schematic illustration of the working mechanisms when (a) s-polarized and (b) p-polarized light rays are incident on the passive PDLC film.

3.2. Fabrication and characterization

A PDLC precursor mixture was developed, consisting of 48.60 wt% BL038 (Merck; birefringence $\Delta n = 0.27$), 4.88 wt% RM 257 (reactive mesogen) and 46.52 wt% NOA 65 (prepolymer with $n_p = 1.52$). After being injected into a 5-μm VA cell, the PDLC precursor was exposed by UV light with an irradiance of 5 mW/cm^2 for 40 minutes, in the presence of a 4 V/μm electric field. To characterize its selective scattering properties, the passive PDLC was fixed on a rotation stage and set to the center of a glass cylindrical container filled with an index matching oil ($n = 1.58$). The incident light (from a 532-nm laser diode) was perpendicular to the PDLC at the initial state, and the incident angle could then be adjusted by rotating the PDLC. The transmittance is normalized to the case where the PDLC is absent and the collection angle of the detector is 7°. The measured results are plotted in Fig. 3. As expected, the two linear polarizations show different behaviors. The s-polarization maintains a high transmittance (> 80%) in air (corresponding to 0° ~ 40° angles in the medium), while p-polarization starts to be scattered (transmittance < 80%) when the incident angle is larger than 20° in the medium (corresponding to 33° in air). Therefore, using such a PDLC as the transparent projection screen, at least a 66° horizontal FOV with good image quality can be obtained, if the display FOV is not limited by other optical components in the system.

Polarized optical microscopy (POM) images of the passive PDLC are captured and exhibited in Fig. 4. Placed the PDLC between a pair of parallel polarizers (Fig. 4(a)), the LC droplets with several μm sizes can be clearly discriminated. By rotating the polarizers to the orthogonal

Optics EXPRESS

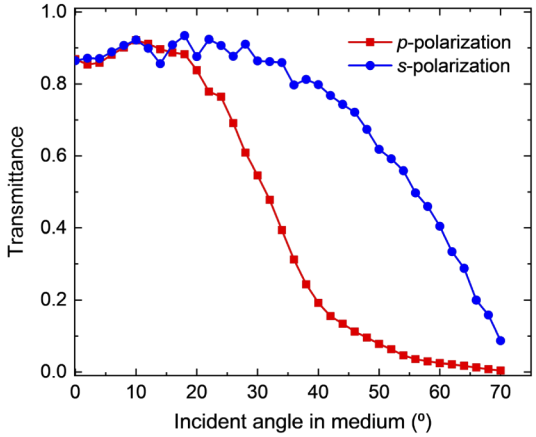

Fig. 3. Angle-dependent transmittance measurements for *p*-polarized (red) and *s*-polarized (blue) input light in a high index medium ($n = 1.58$).

state, the POM image (Fig. 4(b)) turned dark, proving that the normal incident light will mostly transmit through the PDLC without polarization changes.

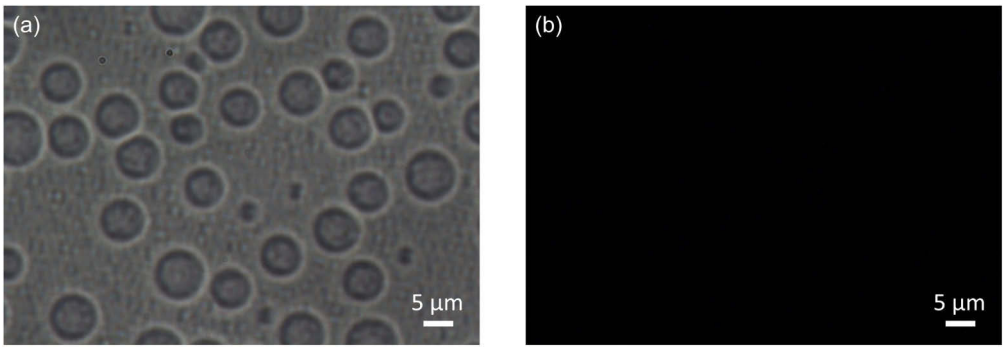

Fig. 4. Captured images of the PDLC under a polarized optical microscope where (a) the polarizers are parallel and (b) the polarizers are perpendicular.

4. Demonstration of a dual-plane display

To prove the feasibility of using the proposed passive PDLC in MFP displays, a dual-plane display as schematically depicted in Fig. 1(a) is built. A commercial LCD (with circularly polarized output light) serves as display panel 1 and a liquid-crystal-on-silicon (LCoS) projector produces an image on the PDLC. The mirror is placed 1.7 cm behind the convex lens ($f = 20$ cm). The distance between the PDLC and the lens is 7 cm and that between the LCD and lens is 9.5 cm. The total volume of the system is about 12×5×5 cm^3, and the system has good tolerance for assembly and calibration. Figure 5 shows two photos captured in front of the beam splitter. "UCF" letters are projected onto the PDLC and "LCD" letters are displayed on the LCD. The focal plane generated by the PDLC TPD is at ~0.4 m (with a magnification of ~3×) and that generated by the LCD is at ~1 m (with a magnification of ~8×). The "UCF" characters have slightly different image sharpness, due to the limited depth of focus of the LCoS projector. Two real objects with distance indicators are placed behind the beam splitter to show the depth difference between these two planes. The constructed dual-focal plane display can easily achieve full color operation

Optics EXPRESS

within 10° FOV, while the image on the LCD will not be blurred by the PDLC. It should be pointed out that the total power efficiency of the PDLC TPD in the system is not high (~2.5%) for two reasons: 1) the relatively low scattering efficiency of the PDLC in the desired direction, and 2) the use of a beam splitter. Further improving the scattering efficiency will be crucial.

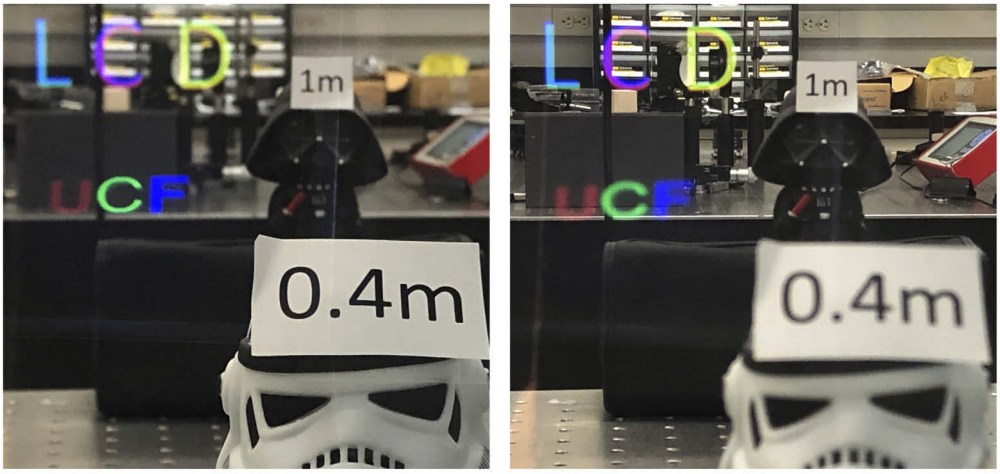

Fig. 5. Photos captured through the dual-plane display prototype, where the camera focuses at around (a) 0.4 m and (b) 1 m in front of the beam splitter.

In principle, more focal planes can be constructed by inserting more PDLC TPDs into the system. But a common issue in TPD-type multi-focal plane displays is that the transmittance of the farthest displays will be greatly reduced. Consequently, the display brightness needs to be enhanced. Another concern is the image quality degradation after passing through multiple TPDs. Since the image blur comes from the scattered light, if only a tiny portion of the scattered light enters human eye, the image quality should remain good. In [23], a four-plane display based on polymer network liquid crystal TPD has been demonstrated with ~90% transmittance of each layer, and its image quality remains decent. Consequently, similar image quality can be expected in our case if more PDLC TPDs are utilized.

5. Conclusion

We have demonstrated an MFP display using a passive PDLC. The passive PDLC is highly transparent for a large range of incident angles in air, but strongly scattering at large oblique angles in high refractive index medium (e.g. glass). To prove the concept, a birdbath architecture has been applied to demonstrate a dual-focal plane see through near-to-eye display. The proposed method can avoid temporal multiplexing and easily achieve high transparency (>85% within ± 33° horizontal FOV in air), full color imaging.

Funding

Air Force Office of Scientific Research (FA9550-14-1-0279).

Disclosures

The authors declare no conflicts of interest.

Optics EXPRESS

References

1. J. Geng, "Three-dimensional display technologies," Adv. Opt. Photonics **5**(4), 456–535 (2013).
2. B. Lee, "Three-dimensional displays, past and present," Phys. Today **66**(4), 36–41 (2013).
3. G. Kramida, "Resolving the vergence-accommodation conflict in head-mounted displays," IEEE Trans. Vis. Comput. Graph. **22**(7), 1912–1931 (2016).
4. H. Hua, "Enabling focus cues in head-mounted displays," Proc. IEEE **105**(5), 805–824 (2017).
5. D. M. Hoffman, A. R. Girshick, K. Akeley, and M. S. Banks, "Vergence–accommodation conflicts hinder visual performance and cause visual fatigue," J. Vis. **8**(3), 33 (2008).
6. M. Lambooij, M. Fortuin, I. Heynderickx, and W. IJsselsteijn, "Visual discomfort and visual fatigue of stereoscopic displays: A review," J. Imaging Sci. Technol. **53**(3), 030201 (2009).
7. S. Liu and H. Hua, "A systematic method for designing depth-fused multi-focal plane three-dimensional displays," Opt. Express **18**(11), 11562–11573 (2010).
8. X. Hu and H. Hua, "High-resolution optical see-through multi-focal-plane head-mounted display using freeform optics," Opt. Express **22**(11), 13896–13903 (2014).
9. G. Tan, T. Zhan, Y. H. Lee, J. Xiong, and S. T. Wu, "Polarization-multiplexed multi-plane display," Opt. Lett. **43**(22), 5651–5654 (2018).
10. Q. Chen, Z. Peng, Y. Li, S. Liu, P. Zhou, J. Gu, J. Lu, L. Yao, M. Wang, and Y. Su, "Multi-plane augmented reality display based on cholesteric liquid crystal reflective films," Opt. Express **27**(9), 12039–12047 (2019).
11. T. Zhan, J. Zou, M. Lu, E. Chen, and S. T. Wu, "Wavelength-multiplexed multi-focal-plane see-through near-eye displays," Opt. Express **27**(20), 27507–27513 (2019).
12. T. Zhan, J. Xiong, J. Zou, and S. T. Wu, "Multifocal displays: review and prospect," PhotoniX **1**(1), 10 (2020).
13. D. Dunn, C. Tippets, K. Torell, P. Kellnhofer, K. Akşit, P. Didyk, K. Myszkowski, D. Luebke, and H. Fuchs, "Wide field of view varifocal near-eye display using see-through deformable membrane mirrors," IEEE Trans. Visual. Comput. Graphics **23**(4), 1322–1331 (2017).
14. N. Padmanaban, R. Konrad, T. Stramer, E. A. Cooper, and G. Wetzstein, "Optimizing virtual reality for all users through gaze-contingent and adaptive focus displays," Proc. Natl. Acad. Sci. U. S. A. **114**(9), 2183–2188 (2017).
15. S. Lee, Y. Jo, D. Yoo, J. Cho, D. Lee, and B. Lee, "Tomographic near-eye displays," Nat. Commun. **10**(1), 2497 (2019).
16. D. Lanman and D. Luebke, "Near-eye light field displays," ACM Trans. Graph. **32**(6), 1–10 (2013).
17. F. C. Huang, K. Chen, and G. Wetzstein, "The light field stereoscope: immersive computer graphics via factored near-eye light field displays with focus cues," ACM Trans. Graph. **34**(4), 1–12 (2015).
18. K. Wakunami, P.-Y. Hsieh, R. Oi, T. Senoh, H. Sasaki, Y. Ichihashi, M. Okui, Y.-P. Huang, and K. Yamamoto, "Projection-type see-through holographic three-dimensional display," Nat. Commun. **7**(1), 12954 (2016).
19. G. Li, D. Lee, Y. Jeong, J. Cho, and B. Lee, "Holographic display for see-through augmented reality using mirror-lens holographic optical element," Opt. Lett. **41**(11), 2486–2489 (2016).
20. J. P. Rolland, M. W. Kureger, and A. Goon, "Multifocal planes head-mounted displays," Appl. Opt. **39**(19), 3209–3215 (2000).
21. S. Lee, C. Jang, S. Moon, J. Cho, and B. Lee, "Additive light field displays: realization of augmented reality with holographic optical elements," ACM Trans. Graph. **35**(4), 1–13 (2016).
22. Y.-H. Lee, H. Chen, R. Martinez, Y. Sun, S. Pang, and S. T. Wu, "Multi-image plane display based on polymer-stabilized cholesteric texture," SID Symp. Dig. Tech. Paper **48**(1), 760–762 (2017).
23. S. Liu, Y. Li, P. Zhou, Q. Chen, and Y. Su, "Reverse-mode PSLC multi-plane optical see-through display for AR applications," Opt. Express **26**(3), 3394–3403 (2018).
24. J. W. Doane, A. Golemme, J. L. West, J. B. Whitehead Jr., and B. G. Wu, "Polymer dispersed liquid crystals for display application," Mol. Cryst. Liq. Cryst. **165**(1), 511–532 (1988).
25. J. Doane, N. Vaz, B. G. Wu, and S. Žumer, "Field controlled light scattering from nematic microdroplets," Appl. Phys. Lett. **48**(4), 269–271 (1986).
26. Y. H. Lin, H. W. Ren, and S. T. Wu, "High contrast polymer-dispersed liquid crystal in a 90° twisted cell," Appl. Phys. Lett. **84**(20), 4083–4085 (2004).
27. G. P. Montgomery, "Angle-dependent scattering of polarized light by polymer-dispersed liquid-crystal films," J. Opt. Soc. Am. A **5**(4), 774–784 (1988).
28. N. A. Vaz, G. W. Smith, and G. P. Montgomery Jr., "A light control film composed of liquid crystal droplets dispersed in a UV-curable polymer," Mol. Cryst. Liq. Cryst. (Phila. Pa.) **146**(1), 1–15 (1987).
29. J. Jiang, G. McGraw, R. Ma, J. Brown, and D. K. Yang, "Selective scattering polymer dispersed liquid crystal film for light enhancement of organic light emitting diode," Opt. Express **25**(4), 3327–3335 (2017).
30. Z. He, K. Yin, E. L. Hsiang, and S. T. Wu, "Volumetric light-shaping polymer-dispersed liquid crystal films for mini-LED backlights," Liq. Cryst. (2020). DOI: 10.1080/02678292.2020.1735546